

# Analytical study of ultrasonic vibration effect on forced insertion process

## 圧入加工における超音波加振効果の解析的検討

Watanabe Yusuke<sup>1†</sup>, Manabu Aoyagi<sup>1</sup>, Hideki Tamura<sup>2</sup>, and Takehiro Takano<sup>2</sup>  
(<sup>1</sup>Muroran Institute of Technology, <sup>2</sup>Tohoku Institute of Technology)  
渡邊 侑佑<sup>1†</sup>, 青柳 学<sup>1</sup>, 田村 英樹<sup>2</sup>, 高野 剛浩<sup>2</sup> (<sup>1</sup>室蘭工大・院; <sup>2</sup>東北工大・工)

### 1. Introduction

An ultrasonically forced insertion (USFI) process can reduce the amount of necessary insertion force. On an early stage in the study of the USFI process, experimental considerations have mainly been carried out.<sup>1,2)</sup> In our previous report, by a finite element analysis (FEA) simulation, it is clarified that a contact stress is reduced by the ultrasonic vibration displacement in the diameter direction.<sup>3)</sup>

The purpose of this study is to quantitatively estimate the effect of the ultrasonic vibration on the USFI process and also to apply it to develop a USFI device with good performance. This paper describes various FEA simulation results of a contact stress on a metal rod and plate under several conditions that are not treated in previous report.<sup>3)</sup> From analysis results, the effect of friction reduction by vibration amplitude and frequency, and the vibrational behavior of an inserted rod were considered.

### 2. Analysis Condition

An analysis model and boundary conditions are shown in Fig.1. Table I shows the parameters of the model and constants used for the analysis. This model has axial symmetry in the central axis ( $R=0$ ). The diameter of the rod is a little larger than that of the hole. The clearance is  $-1 \mu\text{m}$ . This insertion level is defined as “Driving” by Japanese Industrial Standards (JIS). The friction coefficient  $\mu$  is defined by

$$\mu = \mu_d + (\mu_s - \mu_d)\exp(-\beta v), \quad (1)$$

where  $\mu_d$  and  $\mu_s$  are the coefficients of dynamic friction and static one, respectively,  $\beta$  is the damping coefficient,  $v$  denotes the relative velocity of the metal rod and plate.<sup>4)</sup>

FEA simulations were carried out under the conditions that the rod moved by the vibrational displacement  $D_t$ ,

$$D_t = v_a t + a \cdot \sin(2\pi f t), \quad (2)$$

where  $v_a$  is thrust velocity,  $a$ , vibration amplitude,  $f$ , frequency, and  $t$ , time.

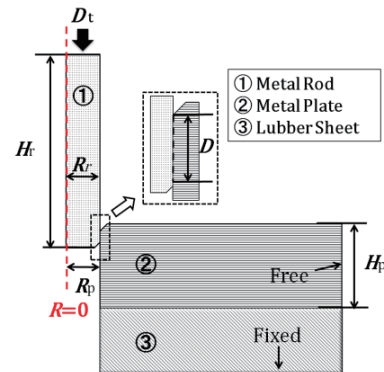


Fig.1 Definition of analysis model.

Table I Parameters of model and constants used for FEA.

$2R_r$	Diameter of metal rod (mm)	12.001
$H_r$	Height of metal rod (mm)	23
$2R_p$	Diameter of hole (mm)	12.000
$H_p$	Height of metal plate (mm)	10
$L_p$	Length of metal plate (mm)	30
$D$	Insertion depth (mm)	1.0
$\mu_d$	Coefficient of dynamic friction	0.3
$\mu_s$	Coefficient of static friction	0.06
$\beta$	Damping coefficient	0.3
$v_a$	Thrust velocity (mm/s)	2.0
$a$	Amplitude of vibration ( $\mu\text{m}$ )	1.0
$f$	Frequency (kHz)	28
$t$	Time of vibration ( $\mu\text{s}$ )	400

### 3. Stress Analysis

#### 3.1 Stress Distribution near the contact surface

Figures 2(a) and 2(b) show the distributions of von Mises stress near the contact surface of the metal rod and the plate at insertion inlet when the rod moved and vibrated at the contact position of 1.0 mm. In the case that the vibration displacement of the rod was the same as the insertion direction, the maximum stress was 67 MPa. On the contrary, in the case that they were in the opposite direction, the maximum stress reduced 38 MPa. Hence it can be considered that the rod is inserted relatively easily when its vibrational motion is opposite to the insertion direction.

Figure 3 shows the locus of x-y displacement on the side of the rod at insertion inlet. The locus drew

an ellipse. The end of rod also made the elliptic motion. The stress became larger when the rod had the displacement in the insertion direction, which contracted in the radial direction, and it was smaller when the rod moved back and expanded.

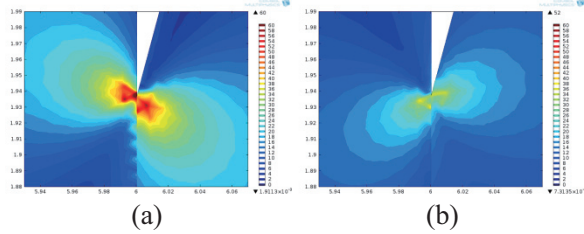


Fig.2 Von Mises stress near contact surface in the case that vibration displacement and insertion are: (a) in the same direction and (b) opposite one.

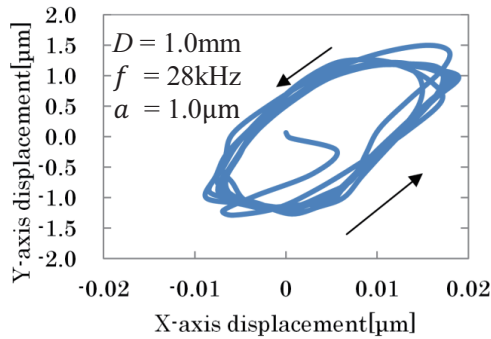


Fig.3 Displacement locus of metal rod at insertion inlet.

### 3.2 Effect of vibration amplitude

Figure 4 shows the effect of vibration amplitude on average contact stress. The contact stress decreased with increase in vibration amplitude. This fact means that the duration of contact stress in low relatively increases with increase in amplitude. A 48% reduction in average contact stress was obtained at the amplitude of 20μm.

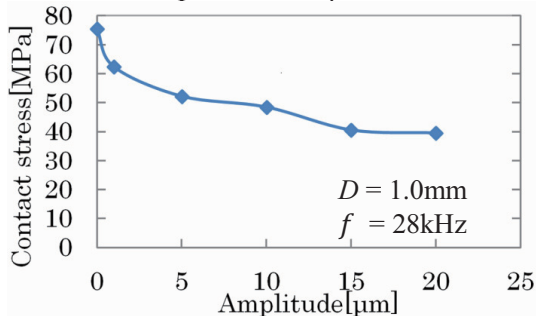


Fig.4 Vibration amplitude to average contact stress.

### 3.3 Effect of vibration frequency

Figure 5 shows the effect of vibration frequency on average contact stress. The contact stress decreased with increase in vibration frequency. However, the effect was hardly seen above 40 kHz. The process in low frequency is desirable considering the production of a high power vibrator.

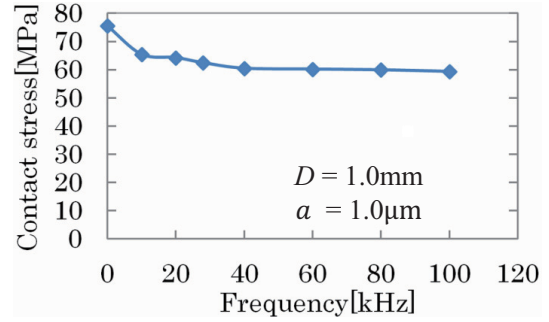


Fig.5 Vibration frequency to average contact stress.

### 4. Sectional strain of metal rod

Figure 6 shows the axial principal strains of the metal rod at insertion inlet and its tip. The principal strains concentrated at the contact surface. The strain near the end of rod was larger than that at insertion inlet, because the hole is expanded by the end of the rod.

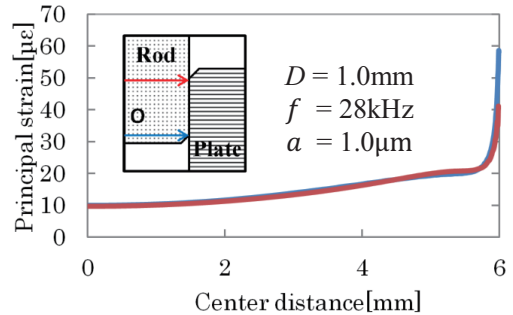


Fig.6 Distribution of principal strain in metal rod.

### 5. Conclusion

- The side of the rod had an elliptic motion. It is considered that a stress on contact surface became larger when the rod contracted in the radial direction, and that the stress decreased when the rod expanded.
- The contact stress decreased with increase in vibration amplitude.
- The influence of the vibration frequency on the contact stress was less than the effect of the vibration amplitude.
- A principal strain concentrated at the surface of the rod, and that near the end of rod was larger than that at insertion inlet.

### Reference

1. N.Saito, N.Mohri, M.Takiguchi: JSPE.(1986) 03:606-611. [in Japanese]
2. N.Mohri, N.Saito: Adv. Manuf. Technol.(1994) 9:225-230.
3. S. Ono, M. Aoyagi, H. Tamura, and T.Takano: Jpn. J. Appl. Phys. 51 (2012) 07GE08.
4. D. J. Benson and J. O. Hallquist John: Comput. Method Appl. M. 78 (1990) 141.